6-2013

Nanodielectric Properties of High Conductivity Carbon-Loaded Polyimide Under Electron-Beam Irradiation

Amberly Evans

J. R. Dennison
Utah State University

Gregory Wilson

Justin Dekany

Nanodielectric Properties of High Conductivity Carbon-Loaded Polyimide Under Electron-Beam Irradiation

USU Materials Physics Group

Amberly E Jensen, JR Dennison, Justin Dekany and Gregory Wilson

Utah State University, Logan, UT 84332-4414

Phone: (435) 363-4704, E-mail: amb.eva@aggiemail.usu.edu

Introduction

High conductivity Black Kapton™ (HCBK) is a common nanodielectric composite material, with an insulating polyimide matrix loaded with nanoscale turbostratic carbon particles to increase its electrical and thermal conductivity. On a macroscopic scale, HCBK acts as a good conductor, with conductivities ranging from 10^{-7} to 10^{-3} $(\Omega\text{-cm})^{-1}$ depending on the fraction of carbon-loading. However, on the nanoscale the material exhibits both conducting and dielectric properties. The length scale is set by the size of the turbostratic carbon soot particles (~100-500 nm) and the carbon-depleted surface regions (~100-5000 nm depth) with separation of carbon-depleted regions (~3000-5000 nm) as shown in Fig. 1(a). This range of separation distances is comparable to the penetration depths of ~0.5-25 keV electrons into the composite of 800 to 11,000 nm (see Fig. 1(b)).

Charging studies on polymers and carbon composites have revealed that sample arcing and luminescence occur as a result of electron beam bombardment. Both insulating regions and electrically isolated carbon particles (floating conductors) can accumulate and dissipate charge; cathodoluminescence results from the insulating polyimide regions. These results have important consequences wherever Black Kapton™ is used in a charging environment—particularly at low temperature vacuum environments where charge dissipation is minimized—such as for spacecraft charging concerns in the space industry where HCBK use is ubiquitous. Arcing can damage the electrical components of a spacecraft causing malfunctions to occur. Luminescence, if intense enough, could potentially produce optical contamination detrimental to the performance of observatory optical elements and sensors, and act to limit their sensitivity and performance windows. As future space observatory missions push the envelope into more extreme environments and use more complex and sensitive detectors, a fundamental understanding of the dependencies of arcing and luminescent intensity on time, temperature, incident electron flux and energy, and material structure becomes critical.

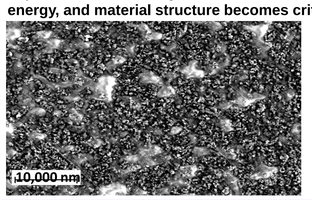

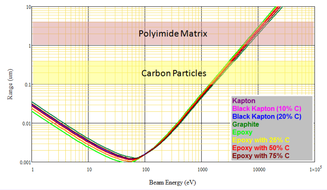

Figure 1. (a) Scanning electron micrograph of HCBK (Kapton™ 275XC230) showing ~0.1 um to 0.5 um diameter graphitic carbon black particles (darker areas) in a polyimide matrix with 1 um to 5 um diameter regions with no carbon particles near the surface (lighter areas). Image acquired at NASA Goddard Space Flight Center with an environmental SEM using a 5 kV beam. (b) Penetration range of graphite and polyimide versus incident electron energy [Wilson, 2012, IEEE-TPS]. Size distributions of carbon particles (red) and insulating matrix (yellow) are shown for comparison.

Abstract

Electron irradiation experiments were conducted to investigate the electron transport, charging, discharging, cathodoluminescence and emission properties of high-conductivity carbon-loaded polyimide (Black Kapton™). We discuss how these results are related to the nanoscale structure of the composite material. Measurements were conducted in an ultrahigh vacuum electron emission test chamber from <40 K to 290 K, using a monoenergetic beam with energies ranging from 3 keV to 25 keV and flux densities from 0.1 nA/cm^2 to 100 nA/cm^2 to deposit electrons in the material surface layer. Various experiments measured transport and displacement currents to a rear grounded electrode, absolute electron emission yields, absolute electron-induced photon emission yields and photon emission spectra (~250 nm to 1700 nm), and arcing rates and location. Numerous arcing events from the material edge to an electrically isolated grounded sample holder (particularly at lower temperatures) were observed, which are indicative of charge accumulation within the insulating regions of the material. Three types of light emission were also observed: (i) short duration (<1 s) arcing, (ii) long duration cathodoluminescence and (iii) intermediate duration (~100 s) glow. We discuss how the electron currents and arcing, as well as light emission absolute intensity and frequency, depend on electron beam energy, power, flux and temperature.

Summary of Results

All types of Black Kapton™ samples studied exhibited readily observable electrical discharges and luminescence when subjected to electron beam bombardment, as illustrated in Fig. 3. Three types of light emission with simultaneous current signatures were observed: (i) short duration (<1 s) arcing resulting from electrostatic discharge, (ii) long-duration sustained glow (cathodoluminescence) that turned on and off with the electron beam, and (iii) intermediate duration (~10-100 s) glow that dissipated exponentially with time after infrequent and rapid onset. Each was detected in the electrometer, oscilloscope, Vis SLR camera, Vis/NIR CCD video camera, and NIR InGaAs video camera; coincidence was almost always seen, except when the signals were below detection thresholds for specific instruments.

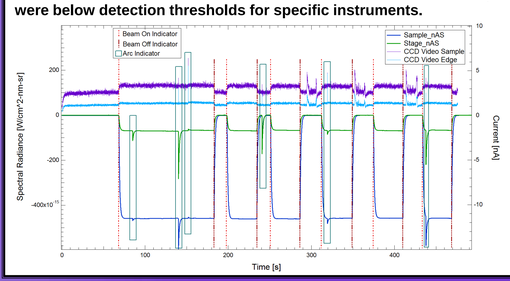

Figure 3. Absolute spectral radiance of the CCD visible video camera from the sample surface (purple curve) and edge (light blue) regions, respectively, plotted against elapsed time. Electrometer current data for the sample (dark blue curve) and stage (green curve), respectively, plotted against elapsed time. The times for electron beam-on (orange dotted vertical lines) and beam-off (brown dashed vertical lines) and arcs (sharp peaks enclosed in the turquoise boxes) are indicated. The noisy signals in the later three beam-off periods are due to extraneous external light sources. Most arcs are seen in both the electrometer and video data.

Experimentation

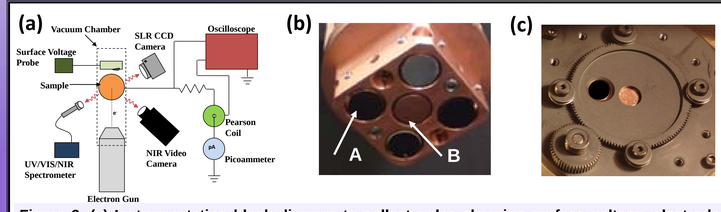

Figure 2. (a) Instrumentation block diagram to collect pulse charging surface voltage, electrode current and cathodoluminescence data induced by electron beam bombardment. Instrumentation includes: picoammeters, Pearson coils, and a storage oscilloscope for electrode current measurements and UV/VIS and NIR spectrometers, an SLR CCD still camera, and a NIR video camera for optical measurements. (b) Sample mount with four samples (A) in corners of the sample holder and a centered copper pseudo Faraday cup (B) for monitoring beam current. (c) Rotating sample cover, exposing only the sample under investigation to the beam.

Conclusions

High conductivity carbon-loaded polyimide underwent electron irradiation experiments to investigate the electron transport, charging, discharging, cathodoluminescence and emission behavior. These experiments revealed that for many applications HCBK cannot be viewed as a macroscopic conductor; it is a nanodielectric. This composite material is comprised of an insulating polyimide matrix with imbedded nanoscale conducting regions. Because the size of these regions is comparable to the length scales of electron penetration and transport, the material exhibits profound changes in its conduction and dielectric properties. Upon electron beam bombardment, the material exhibited behaviors similar to other dielectric materials; these include long duration cathodoluminescence, short duration arcing, and intermediate duration flare behaviors. As shown here, these properties can only be understood quantitatively by considering the nanoscale structure.

Acknowledgements

Project support was from NASA Goddard Space Flight Center and a NASA Graduate Research Fellowship.

Results

Arcs

HCBK exhibited numerous short duration (<1 s) electrostatic discharge or arcing events, as seen in Fig. 4. Analysis of individual frames of camera data (see Fig. 4) allowed determination of the location of each arc, with a spatial resolution of <100 μm; these were (almost exclusively) in the high electric field region within the gap between the sample edge and adjacent electrically-isolated grounded sample holder.

Lower temperature samples in general showed larger arc rates, although insufficient data have been acquired at different beam current densities and energies to establish a functional dependence. The dark current and radiation induced conductivities in polyimide are several orders of magnitude lower at the lower temperatures, leading to reduced charge dissipation and enhanced charging and electrostatic discharges at low temperatures.

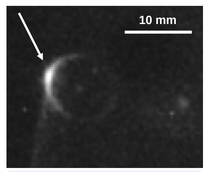

Figure 4. Arrow indicates arc position on sample.

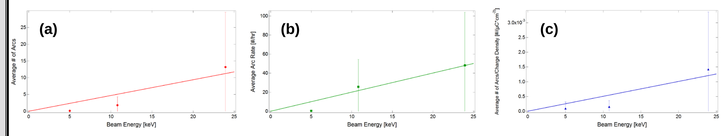

Figure 5. From electrometer data, the dependence of (a) number of arcs, (b) arc rate, and (c) average arc rate scaled by beam current density (or equivalently, number of arcs per deposited charge density) as a function of beam energy. Each of these displays an increase with increasing beam energy, although there are insufficient data with large error bars to determine if there are specific functional dependences for any of these cases. There is not a clear trend for the dependence of arc rate on incident current density. Enhanced tests, including os sample size, are currently underway.

Sustained Glow

Sustained glow is long duration cathodoluminescence that turns on and off with the incident electron beam. It occurs over the full illuminated ~1 cm^2 sample area when beam is on, as seen in Fig. 6. Fig. 3 above shows that there is excellent temporal correlation between the electrometer data and the video camera spectral radiance curves. Sustained glow intensity or current takes a finite amount of time to reach a fairly steady equilibrium value. There is also a finite decay time seen in glow intensity and current curves after the beam is turned off. The exponential rise and decay time constants (10^{-1} s) are roughly the same and are believed to be related to filling and release rates of the traps in the insulating polyimide.

Simple models based on the disordered bandstructure predict (see Fig. 7(a)) that luminescence increases linearly with incident power density (beam energy times beam current density) for non-penetrating radiation (*e.g.*, M55J carbon/epoxy composite data) and decreases in proportion to the range of incident electrons for penetrating radiation (*e.g.*, fused silica coating data). The spectral radiance of HCBK samples is largely independent of absorbed power. A linear combination of thick polyimide regions (with non-penetrating radiation) and thin polyimide layers coating near-surface carbon particles (with penetrating radiation) can produce such a signature nearly independent of incident power. The fraction of such regions can be approximated, respectively, as the fraction of light (~36%) and dark (~64%) pixels in a binary image of the electron micrograph of Fig. 1. This simple luminescence model for 10 nm (~0.4 keV penetration energy) and 50 μm (~60 keV penetration energy) in the ratio of thin to thick areas approximated by the SEM binary image predicts the curve of spectral radiance versus energy shown.

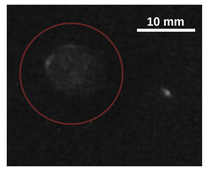

Figure 6. The sustained glow of HCBK while the electron beam (inside red circle) is on .

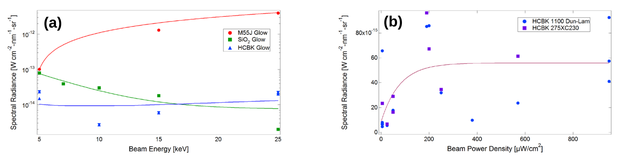

Figure 7. Predictions of the absolute spectral radiance for two types of HCBK materials (230XC275 and 1100 Dun-Lam™ HCBK/Kevlar™/HCBK laminate) based on luminescence models of disorderd bandstructure (Evans, 2013, IEEE-TPS, in press). (a) Versus incident energy. (b) Versus incident beam power density.

Flares

Features seen simultaneously in current and VIS and NIR spectral response curves of intermediate duration (~100 s) glow that dissipated exponentially with time have been termed flares (see Fig. 8). Flares are infrequent (~2 flares/hr) and were only observed in long, high flux runs, which suggests the necessity for substantial charging within the sample before flares can occur.

Flares (usually) have an arc associated with their instigation, although the origin of such large arc triggers is not known (see Fig. 9). Flares have abrupt onset rise times (<0.1 s), believed to be associated with a rapid discharge. Flares also exhibit very long times (10^2 s) for the currents or spectral radiance to return to pre-flare equilibrium values associated with sustained glow. The response for individual flares between the abrupt onset and long term decay is complex and can vary from one flare to the next.

The spectral response and electrometer currents (~1-100 nA amplitude with <1-10 μJ) of flares are ~2-20X that observed for typical sustained glow. Only about a half a dozen flares have been observed in ~20 hrs of HCBK data, too few to accurately determine the flare dependence on current density, charge fluence, beam energy, or deposited power. Flares seem to occur mostly for higher energies or power density; this suggests a possible link with charge dissipation through RIC. RIC allows lateral charge motion and vertical motion in the penetration region.

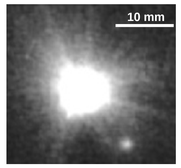

Figure 8. A video frame containing a flare event.

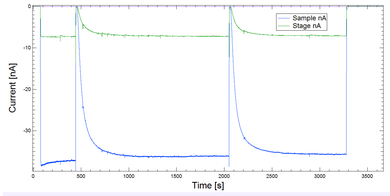

Figure 9. Electrometer response of a flare event indicated by the boxes.